Supplemental Information

A. Supplemental Figure Legends

Figure S1: Quantification of nuclear (genomic) DNA separated from protein for silver stain shows equal numbers of isolated nuclei per sample. (A-B) Nuclei were isolated (using a cytoplasmic membrane-specific lysis buffer from the PARIS kit, Life Technologies) from equal numbers of cultured cells that had been infected with control shRNA or *Xpo7*-shRNA, as well as wt sorted extruded nuclei (EN). Then, gDNA was separated from protein in each sample using nondenaturing lysis buffer with high salt (1% (w/v) Triton x100, 50mM Tris-HCl pH 7.4, 300 mM NaCl, 5mM EDTA) followed by sonication. gDNA was isolated with 100% ethanol precipitation, then washed with 75% ethanol. EN were treated the same as all other samples (including lysis of the sorted sample to remove remaining cytoplasmic membrane surrounding extruded nuclei). (A) gDNA from each pellet was quantified by qPCR with primers against the housekeeping gene HPRT. The gDNA was first quantified using the Nanodrop machine (Thermo Scientific) in order to load equal amounts in each PCR reaction and the 260/280 ratios were consistently above 1.80. Note that the C_t value (threshold cycle) is lowest for EN, corresponding to more DNA, but the three samples are not statistically different from each other. Each point corresponds to a biological replicate of 3 million cells, which provided sufficient protein for the SDS protein gel in Figure 1A. (B) The nuclear samples were also quantified for protein using the Bio-Rad DC Protein Assay (modified Lowry) and, consistent with the quantities seen on silver stain, protein isolated from EN samples had considerably less protein per nucleus than those from control cells or *Xpo7*-KD cells at 48hrs. Concentration shown is ng/ul measured at 750nm per Bio-Rad DC Assay protocol.

Figure S2: Nuclear proteins such as histones are exported from the nucleus during normal erythroid differentiation. (A) Erythroblasts cultured in Epo-containing media with and without proteasome inhibitor MG132 given at 24

hours were harvested after 24 and 48 hours and then fractionated into cytoplasmic and nuclear extracts using the PARIS Isolation Kit (Life Technologies). Immunoblotting was performed against a cytoplasmic protein (GAPDH), nuclear protein histone H3 acetyl-lysine 27 (H3K27Ac), and total histone H2A. Hi, long exposure of blot, 10 min. Lo, short exposure of blot, 5 sec. (B-C) Immunofluorescence (IF) of cultured erythroblasts at 48 hours of culture showing migration of nuclear proteins into the cytoplasm before and during enucleation. Primary antibodies are against histones (B): Histone 1, Macro histone H2A.1, and pan-methyl Histone H3 on lysine 9; or nuclear histone methyltransferases (HMTs) (C): ESET, G9, and Suv39-H1. Blue staining is against DNA using DAPI. Secondary antibodies used were Alexa-594 conjugated secondary antibody (macro H2A.1 and pan-methyl H3K9) or Alexa-488 conjugated secondary antibody (H1 and three HMTs). In all panels, scale bar=10 μm.

Figure S3: Expression of Importins, Exportins, and other Ran-binding proteins in wild-type fetal liver erythroblasts. (A) Erythroid progenitors were isolated (time 0) and then cultured in the presence of Epo. Erythroblasts were then harvested at 24 and 48 hours of culture and immunoblotting was performed against GAPDH and the most abundant exportins (*Xpo7* and *Xpo5*) and importins (alpha, or *Kpna2*, and beta, or *Kpnb1*). Antibody Xpo7a was raised against XPO7 with the previously annotated first exon (Exon 1a, Figure 2) and Xpo7b against XPO7 with the erythroid first exon (Exon 1b, Figure 2). Note that only the erythroid-specific Xpo7b is abundant during erythroid differentiation. (B) RNA-seq levels (from [1]) of important *Ran* and *RanGAP* transcripts during murine definitive erythropoiesis. Note that while all these transcripts decrease during erythropoiesis, they are still present at considerable levels (on the level of 100 reads), reflecting that there is still some expression of these genes late in red cell development that would allow nuclear transport to occur.

Figure S4: Expression profiling in human and mouse tissues shows *Xpo7* expression is highly erythroid-specific. Microarray expression profiling of 79 human and 61 mouse tissues reveals that *Xpo7* displays a highly erythroid-specific tissue expression pattern (Novartis BioGPS database; dataset GeneAtlas U133A). Three tissues showing highest expression levels are bone marrow, fetal liver, and CD71+ erythroblasts. Note that this expression pattern is common to other highly erythroid-specific genes such as *GATA1* or *Alas2*.

Figure S5: The erythroid-specific first exon of *Xpo7* utilizes an erythroid-specific promoter. Genome browser depicting the genomic structure of the *Xpo7* gene, showing RNAseq tracks (grey and black), Refseq gene annotations (blue, and location analysis tracks from ENCODE (brown) for histone marks trimethyl-H3K4, trimethyl-H3K36, and trimethyl-H3K27, and transcription factors (TFs) GATA1 and Tal1 in erythroblasts. Note that the previously annotated (nonerythroid) first exon (blue box) shows higher expression in earlier progenitors but very little transcript in late TER119+ erythroblasts and almost no TF binding in either G1E cells or primary erythroblasts. The erythroid-specific first exon (red box) shows evidence of utilizing a nearby (intronic) promoter, including trimethyl-H3K4 and GATA1 and Tal1 binding as well as trimethyl-H3K36 (light blue arrow): showing elongation of the *Xpo7* transcript downstream of the erythroid-specific promoter (red box) but not the region immediately downstream of the nonerythroid promoter (blue box). GATA1 binding appears to be directly induced in G1-ER cells upon GATA1 reintroduction[2] near the erythroid but not the nonerythroid start site (bottom two tracks, red box). Blue and red boxes are 10kB in width.

Figure S6: No difference in either apoptosis or cell cycle arrest after *Xpo7* knockdown. (A) Measurement of apoptosis using FACS analysis of 7-AAD and Annexin-5 stained erythroblasts infected with either *Xpo7* or control shRNA. Percent apoptotic cells (Annexin-5-positive and 7-AAD low) are shown as culture time progresses. There is no significant difference in apoptosis between control

and *Xpo7*-knockdown cells. (B) Cell cycle status (G1) of erythroblasts infected with either *Xpo7* or control shRNA over the course of 48-hr *in vitro* culture. Note how the majority of wild-type erythroblasts (red line) have left the cell cycle by 32 hours of culture, and *Xpo7*-knockdown cells display the same phenomenon.

Figure S7: No difference in acquisition of cell surface marker TER119 after *Xpo7* knockdown. (A,B) Cultured erythroblasts were examined by FACS for TER119 and CD71 staining after culture for 48 hours in Epo-containing media. Representative dotplot (A) or TER119 histogram (B) showing the majority of cells with either control shRNA or *Xpo7* knockdown acquired significant TER119 after 48 hours.

Figure S8: Significant inhibition of enucleation after *Xpo7* knockdown; cells do not catch up after additional time in culture. (A) Quantification of 5 experiments shown in Figure 3C, normalized to the percentage of enucleated cells in control sample. Note the more significant inhibition of enucleation by the construct sh*Xpo7*-1, which was used in all further studies. (B) Enucleation measured by FACS of wt cultured erythroblasts using DAPI and TER119 staining (as in [3]) at 48 and 72 hours, showing no increase in enucleation after 48 hours of culture.

Figure S6: Quantification of histone (red) staining outside of nuclear staining. (A) IF images of cultured erythroblasts infected with control shRNA. H2A (red) and DAPI (blue) staining were captured as in Figure 4. (B) Individual channel images were converted to binary (black = positive signal) and the area of red staining which does not colocalize with blue staining was calculated using the NOT (subtract) function of Fiji[4] software (version of ImageJ, http//fiji.sc). Note how red cytoplasmic H2A staining seen in the merged image is quantified as black signal in the resulting binary image (far right). Amount of staining (pixels) was measured using Fiji and quantified only for cells with positive staining in both channels.

B. Supplemental Tables

Table S1. Sequences of Alternative (Erythroid-specific) First Exon of *Xpo7*

First Exon	Sequence
Previously Annotated (1A)	CTGCACATGATCCGCCATTTTGCTCCATTCATGCTCCTCTCAGGCCC CCCCTCCCCACCAGCGCGCACCTCGGCCGGGgccgccgccgccgctgctgc cgccgtcgccgctgcGCCTGCGCGCTGGGGACTCGGCGCGCTACGCTCGT GGCGTAGCGCCGCTCTGCCGCGCAGGCCCCGGCCGGCCGCTCTG GGTTGGAGAATGCGCAGCGTGGCTGGGACGGCGTAGGGGCGCGG GCAACGTCAGCGGCCCGGAGACGCCGGGTGGGAGGAAGCGGAGG GCCGTGGAAGCGCAAGGGAGGGGAGCTGGGGGAACAAAGCTTTGT TTACATGGGTTTTAAAGGGGCCGCGCTCGAACTCGCGCGCGGGCCA GCGCCGCGTGGGAGCGGAGCACGCTGCCTGTCGTTTCGGGTGCTG TCATGGCTCCACCCC
Erythroid-specific (1B)	CTTTCTCCCTGAGTCCCGCATGTCTCAAGTGCAGCACACACTCTTCT GATGTGTTTAAATTCTTGCTTCAGTTCCACATTTAAAGT

Table S2. Significantly Changed Genes after *Xpo7*-knockdown (.xls file)

Tables S3-S4. Significant Proteins Identified in *Xpo7*-knockdown nuclei and extruded nuclei (EN)

Table S3. Proteins Identified in Extruded Nuclei (top 50)

Gene Description Name	Gene	Gene Accession Number	MW	Unique Peptides
histone H2A type 3 [Mus musculus]	*Hist3h2a*	gi|30061353 (+5)	14 kDa	250
histone H2A type 2-A [Mus musculus]	*Hist2h2aa2*	gi|20799907 (+1)	14 kDa	224
histone H1.3 [Mus musculus]	*Hist1h1d*	gi|254588110	22 kDa	223
histone H1.2 [Mus musculus]	*Hist1h1c*	gi|9845257	21 kDa	223
histone H4 [Mus musculus]	*Hist4h4*	gi|23943922 (+11)	11 kDa	222
histone H2B type 1-P [Mus musculus]	*Hist1h2bp*	gi|160420308 (+3)	16 kDa	213
histone H1.4 [Mus musculus]	*Hist1h1e*	gi|13430890	22 kDa	185
lamin-B1 [Mus musculus]	*Lmnb1*	gi|188219589	67 kDa	179
histone H2A.x [Mus musculus]	*H2afx*	gi|7106331	15 kDa	146
histone H1.5 [Mus musculus]	*Hist1h1b*	gi|21426893	23 kDa	128
histone H1.1 [Mus musculus]	*Hist1h1a*	gi|21426823	22 kDa	117
histone H2A.Z [Mus musculus]	*H2afz*	gi|7949045	14 kDa	115
histone H3.3 [Mus musculus]	*H3f3a*	gi|6680159 (+1)	15 kDa	96
prelamin-A/C isoform A [Mus musculus]	*Lmna*	gi|162287370	74 kDa	81

DNA topoisomerase 2-alpha [Mus musculus]	*Top2a*	gi|153945749	173 kDa	75
ubiquitin-40S ribosomal protein S27a [Mus musculus]	*Rps27a*	gi|13195690 (+2)	18 kDa	62
nuclear pore complex-associated protein Tpr [Mus musculus]	*Tpr*	gi|270309140	274 kDa	55
nuclear mitotic apparatus protein 1 [Mus musculus]	*Numa1*	gi|254675300	236 kDa	51
core histone macro-H2A.1 isoform 2 [Mus musculus]	*H2afy*	gi|283945572 (+1)	40 kDa	50
nucleolar protein 58 [Mus musculus]	*Nop58*	gi|120407050	60 kDa	49
nucleolar protein 56 [Mus musculus]	*Nop56*	gi|126090932	64 kDa	45
heterogeneous nuclear ribonucleoprotein L [Mus musculus]	*Hnrnpl*	gi|183980004	64 kDa	37
myb-binding protein 1A [Mus musculus]	*Mybbp1a*	gi|31982724	152 kDa	36
nucleolar RNA helicase 2 [Mus musculus]	*Ddx21*	gi|72384374	94 kDa	29
DNA topoisomerase 1 [Mus musculus]	*Top1*	gi|112734855	91 kDa	28
antigen KI-67 [Mus musculus]	*Mki67*	gi|169234624	351 kDa	26
PREDICTED: nucleophosmin-like [Mus musculus]	*Gm15484*	gi|149251776 (+1)	33 kDa	26
tyrosine-protein kinase BAZ1B [Mus musculus]	*Baz1b*	gi|170295818	171 kDa	26
SWI/SNF-related matrix-associated actin-dependent regulator of chromatin subfamily A member 5 [Mus musculus]	*Smarca5*	gi|40254124	122 kDa	26
actin, cytoplasmic 1 [Mus musculus]	*Actb*	gi|6671509 (+1)	42 kDa	24
nucleolin [Mus musculus]	*Ncl*	gi|84875537	77 kDa	24
DNA topoisomerase 2-beta [Mus musculus]	*Top2b*	gi|34328148	182 kDa	22
lamin-B receptor [Mus musculus]	*Lbr*	gi|229608895	71 kDa	21
lamin-B2 [Mus musculus]	*Lmnb2*	gi|113195686	67 kDa	21
E3 SUMO-protein ligase RanBP2 [Mus musculus]	*Ranbp2*	gi|153792534	341 kDa	21
putative pre-mRNA-splicing factor ATP-dependent RNA helicase DHX15 isoform 2 [Mus musculus]	*Dhx15*	gi|110835723	91 kDa	19
protein RRP5 homolog [Mus musculus]	*Pdcd11*	gi|54607128	208 kDa	19
elongation factor 1-alpha 1 [Mus musculus]	*Eef1a1*	gi|126032329	50 kDa	18
chromobox protein homolog 3 [Mus musculus]	*Cbx3*	gi|108860695 (+3)	21 kDa	18
chromobox protein homolog 1 [Mus musculus]	*Cbx1*	gi|6671696	21 kDa	17
chromobox protein homolog 5 [Mus musculus]	*Cbx5*	gi|116008461 (+2)	22 kDa	17
116 kDa U5 small nuclear ribonucleoprotein component isoform b [Mus musculus]	*Eftud2*	gi|158508674 (+1)	109 kDa	17
lamina-associated polypeptide 2 isoform epsilon [Mus musculus]	*Tmpo*	gi|121949765	50 kDa	16
H/ACA ribonucleoprotein complex subunit 4 [Mus musculus]	*Dkc1*	gi|91064867	57 kDa	16
mesotrypsin-like [Mus musculus]	*Gm10334*	gi|157058298 (+1)	26 kDa	16
ATP-dependent RNA helicase A [Mus musculus]	*Dhx9*	gi|150456419	150 kDa	15
nucleolar and coiled-body phosphoprotein 1 isoform B [Mus musculus]	*Nolc1*	gi|86198327 (+3)	73 kDa	14
PREDICTED: rRNA 2'-O-methyltransferase fibrillarin-like isoform 1 [Mus musculus]	*Fbll1*	gi|149251501 (+1)	34 kDa	14
putative ribosomal RNA methyltransferase NOP2 [Mus musculus]	*Nop2*	gi|158966689	87 kDa	14

Table S4. Proteins Identified in *Xpo7*-Knockdown Nuclei (top 50)

Gene Description Name	Gene	Gene Accession Number	MW	Unique Peptides
antigen KI-67 [Mus musculus]	*Mki67*	gi|169234624	351 kDa	163
prelamin-A/C isoform A [Mus musculus]	*Lmna*	gi|162287370	74 kDa	104
heterogeneous nuclear ribonucleoproteins A2/B1 isoform 1 [Mus musculus]	*Hnrnpa2b1*	gi|109134362 (+1)	36 kDa	79
histone H1.3 [Mus musculus]	*Hist1h1d*	gi|254588110	22 kDa	71
ankyrin-1 isoform 1 [Mus musculus]	*Ank1*	gi|160707915	210 kDa	69
histone H1.2 [Mus musculus]	*Hist1h1c*	gi|9845257	21 kDa	68
spectrin beta chain, erythrocyte [Mus musculus]	*Spnb1*	gi|84490394	268 kDa	68
histone H2B type 1-P [Mus musculus]	*Hist1h2bp*	gi|160420308 (+3)	16 kDa	62
histone H2A type 3 [Mus musculus]	*Hist3h2a*	gi|30061353 (+5)	14 kDa	59
spectrin alpha chain, erythrocyte [Mus musculus]	*Spna1*	gi|19526481	280 kDa	56
myb-binding protein 1A [Mus musculus]	*Mybbp1a*	gi|31982724	152 kDa	52
ubiquitin-40S ribosomal protein S27a [Mus musculus]	*Rps27a*	gi|13195690 (+2)	18 kDa	52
histone H2A type 2-A [Mus musculus]	*Hist2h2aa2*	gi|20799907 (+1)	14 kDa	50
histone H1.4 [Mus musculus]	*Hist1h1e*	gi|13430890	22 kDa	50
nuclear pore complex-associated protein Tpr [Mus musculus]	*Tpr*	gi|270309140	274 kDa	50
DNA (cytosine-5)-methyltransferase 1 isoform 1 [Mus musculus]	*Dnmt1*	gi|327180732	183 kDa	48
histone H1.5 [Mus musculus]	*Hist1h1b*	gi|21426893	23 kDa	47
lamin-B1 [Mus musculus]	*Lmnb1*	gi|188219589	67 kDa	42
splicing factor, proline- and glutamine-rich [Mus musculus]	*Sfpq*	gi|23956214	75 kDa	42
histone H2A.x [Mus musculus]	*H2afx*	gi|7106331	15 kDa	41
myosin-9 isoform 1 [Mus musculus]	*Myh9*	gi|114326446	226 kDa	36
nuclear mitotic apparatus protein 1 [Mus musculus]	*Numa1*	gi|254675300	236 kDa	34
elongation factor 1-alpha 1 [Mus musculus]	*Eef1a2*	gi|126032329	50 kDa	33
heterogeneous nuclear ribonucleoprotein M isoform b [Mus musculus]	*Hnrnpm*	gi|158186704 (+1)	74 kDa	33
heterogeneous nuclear ribonucleoprotein U [Mus musculus]	*Hnrnpul1*	gi|160333923	88 kDa	33
far upstream element-binding protein 2 [Mus musculus]	*Khsrp*	gi|163954948	77 kDa	32
heterogeneous nuclear ribonucleoprotein L [Mus musculus]	*Hnrnpl*	gi|183980004	64 kDa	30
heat shock cognate 71 kDa protein [Mus musculus]	*Hspa8*	gi|31981690	71 kDa	30
lamina-associated polypeptide 2 isoform epsilon [Mus musculus]	*Tmpo*	gi|121949765	50 kDa	29
histone H4 [Mus musculus]	*Hist4h4*	gi|23943922 (+11)	11 kDa	28
histone H2A.Z [Mus musculus]	*H2afz*	gi|7949045	14 kDa	28
structural maintenance of chromosomes protein 1A [Mus musculus]	*Smc1a*	gi|258613892	143 kDa	26
elongation factor 2 [Mus musculus]	*Eef2k*	gi|33859482	95 kDa	26
serine/arginine repetitive matrix protein 2 [Mus musculus]	*Srrm2*	gi|126157504	284 kDa	25
PREDICTED: nucleophosmin-like [Mus musculus]	*Gm15484*	gi|149251776 (+1)	33 kDa	25

actin, cytoplasmic 1 [Mus musculus]	*Actb*	gi|6671509 (+1)	42 kDa	24
probable ATP-dependent RNA helicase DDX5 [Mus musculus]	*Ddx5*	gi|83816893	69 kDa	24
band 3 anion transport protein [Mus musculus]	*Slc4a1*	gi|6755560	103 kDa	23
chromodomain-helicase-DNA-binding protein 4 [Mus musculus]	*Chd4*	gi|39204553	218 kDa	23
nucleolar RNA helicase 2 [Mus musculus]	*Ddx21*	gi|72384374	94 kDa	23
histone H3.3 [Mus musculus]	*H3f3a*	gi|6680159 (+1)	15 kDa	22
elongation factor 1-delta isoform a [Mus musculus]	*Eef1d*	gi|56699438	73 kDa	22
DNA topoisomerase 2-alpha [Mus musculus]	*Top2a*	gi|153945749	173 kDa	21
eukaryotic translation initiation factor 3 subunit A [Mus musculus]	*Eif3a*	gi|146219837	162 kDa	20
nucleolar protein 56 [Mus musculus]	*Nop56*	gi|126090932	64 kDa	20
mesotrypsin-like [Mus musculus]	*Gm10334*	gi|157058298 (+1)	26 kDa	19
histone H1.1 [Mus musculus]	*Hist1h1a*	gi|21426823	22 kDa	18
heterogeneous nuclear ribonucleoproteins C1/C2 isoform 3 [Mus musculus]	*Hnrnpc*	gi|283436180	32 kDa	18
heterogeneous nuclear ribonucleoprotein A1 isoform a [Mus musculus]	*Hnrnpa1*	gi|6754220 (+1)	34 kDa	18

C. Supplemental Experimental Methods:

Erythroid progenitor isolation and culture

Total fetal liver cells were isolated from E14.5 wild-type C57BL/6 embryos (Jackson Laboratory) and then stained with biotin-labeled anti-hematopoietic lineage antibodies (CD3, CD11b, Gr-1, TER-119, B220), additional TER-119 antibody, and hematopoietic stem/progenitor cell antibodies (Sca-1, CD41, CD16/CD32) in order to obtain early erythroid progenitors by streptavidin-conjugated magnetic bead separation (BD Imag, BD Biosciences) as previously described[5]. TER119-negative erythroid progenitors were then cultured in erythropoietin (Epo)-containing medium on fibronectin-coated plates for 48 hours as previously described[6]. All animal studies were approved by the MIT/Whitehead and Yale University Institute Animal Care and Use Committees.

Retroviral constructs

Retroviruses for shRNA were constructed using the MSCV-pgkGFP-U3-U6P-Bbs vector (murine stem cell retroviral vector-pgk promoter-GFP-U6 promoter-shRNA) as described previously[6]. The control shRNA construct was designed

against the firefly luciferase gene. Five candidate shRNA sequences against *Xpo7* were obtained from the online Broad Institute RNAi consortium shRNA library (https://www.broadinstitute.org/rnai/trc/lib, Cambridge, MA); the retroviral construct with the most significant knockdown (over 70%) was used for all experiments where only one knockdown vector is described. H2A-Turquoise fusion experiments (Figure 5C) utilized the vector construct comprised of the MSCV-MIGR1 vector where the GFP gene was replaced by the fusion gene mTurquoise-H2A, an enhanced cyan fluorescent protein fused with histone H2A (obtained from Addgene #36207) (Goedhart et al, 2012).

Generation of retroviral supernatants and infection of primary cells

The retrovirus-packaging cell line 293T was maintained and transfected with retroviral plasmid as previously described[6]. For infection of purified TER119-negative fetal liver cells, $2x10^5$ cells were resuspended in 1mL thawed viral supernatant containing 4 µg/mL Polybrene (Sigma) and centrifuged at 1200 rpm for 1 hour at 25°C as previously described[6]. Aliquots of each sample were harvested at 24 and 48 hours of culture for cell counts using a hemacytometer as well as numerous other studies, described below.

Western blotting and silver staining

Approximately $2x10^6$ GFP+ cells were sorted from each sample after 24, 36, or 48 hours of retroviral infection, and then cytoplasmic and nuclear fractions were separated using the PARIS isolation kit (Life Technologies). The same procedure was also followed for normal cells that had been cultured for 48 hours and had been treated with 5uM proteasome inhibitor MG132 (Enzo Life Sciences) at 24 hours of culture. The nuclear pellet was further disrupted in RIPA buffer with high salt (300mM) by sonication for 3 min using a Bioruptor test tube sonicator (Diagenode) and then boiled for 10 min followed by centrifugation at 14000rpm for 10 min. gDNA was isolated from each pellet with 100% ethanol precipitation, then washed with 75% ethanol. gDNA was first quantified using the Nanodrop

machine (Thermo Scientific) in order to load equal amounts in each PCR reaction and the 260/280 ratios were consistently above 1.80. Lysates were then separated using Novex 4-12% electrophoresis gels (Life Technologies) and either wet transferred onto polyvinylidene fluoride membranes (Immobilon P, Millipore) followed by immunoblotting with the indicated antibodies or analyzed by silver stain (Silverquest kit, Invitrogen).

Antibodies

Xpo7 antibody used in Figure 2 was previously made against the C-terminus in Dr. Gorlich's laboratory[7]. *Xpo7* antibody against the different exon 1 a and 1b isoforms were created using the following N-terminal peptides which were then used in carrier-coupled form to immunize rabbits, and the resulting sera affinity-purified on columns with the respective immobilized peptides:

Xpo7-1A: Acetyl-NH-MADHVQSLC-COOH
Xpo7-1B: NH2-MRDSGRKSC-COOH

Histone-specific antibodies were rabbit polyclonal Histone H2A (#ab18255, Abcam), rabbit polyclonal Histone H3 (#06-755, EMD-Millipore), calf thymus conjugate Histone H1 conjugated to Alexa-488 (H13188, Life Technologies), rabbit monoclonal Pan-Methyl-Histone H3K9 (#44735, Cell Signaling), rabbit polyclonal macro-histone H2A.1 (#ab37264, Abcam), and rabbit polyclonal Histone H3-acetyl K27 (ab4729, Abcam). Mouse monoclonal GAPDH antibody (Clone 6C5) and goat polyclonal Lamin B antibody (M20) were obtained from Santa Cruz Biotechnologies. Lysine Methyltransferase rabbit polyclonal antibodies against ESET (#2196), G9a (#3306), and SUV39H1 (#8729) were obtained from Cell Signaling Technology.

Secondary antibodies used for immunoblotting were: TrueBlot HRP anti-mouse, anti-rabbit, or anti-goat IgG at 1:2000 (eBioscience). Secondary antibody used for immunofluorescence was Alexa Fluor® 594 donkey anti-rabbit (#A21207, Life Technologies). Details of the immunofluorescence staining protocol are included in the Supplemental Experimental Procedures.

Flow cytometric analysis of erythroid differentiation and enucleation, and FACS

Cells were immunostained with allophycocyanin (APC)–conjugated anti-TER119 antibody at 1:200 (BD Pharmingen), phycoerythrin (PE)–conjugated anti-CD71 antibody at 1:200 (BD Pharmingen), and 10μg/ml Hoechst 33342 (Sigma) for 15 min at room temperature. Propidium iodide (Sigma) was added to exclude dead cells from analysis. Flow cytometry and FACS were carried out as previously described[6]. Sorted GFP+ cells were harvested for additional biochemical and molecular studies described below.

Hemoglobin quantification

Mouse fetal liver cells infected with control and *Xpo7* shRNA retroviruses as described above were sorted for GFP at 48 hours of culture and then $2x10^6$ sorted GFP+ cells were lysed in 200μl Drabkin's reagent according to the manufacturer's instructions (Sigma). Spectrophotometric analysis was then performed at 540nm and control samples' intensities were compared to the *Xpo7*-knockdown samples.

Cell cycle and apoptosis assays

Cells were sorted for GFP+ and then prepared for apoptosis and cycle analysis as previously described[6].

RNA isolation and Quantitative Real-Time Polymerase Chain Reaction (qRT-PCR)

RNA was isolated using the RNAeasy Micro kit (Qiagen) from cultured cells 48 hours after retroviral infection (Figure 2), sorted GFP+ cells from each knockdown sample, or from populations R2-R5 (Figure 1) from fetal liver. DNA was obtained via reverse-transcription (Stratagene) and quantitative PCR performed using SYBR green real-time PCR (Applied Biosciences/Life Technologies) as previously described[6]. Primers against erythroid-specific genes are from [6].

Microarray sample preparation, hybridization, and analysis

Total RNA was isolated from control and *Xpo7*-knockdown samples as described. Each samples' cDNA was prepared and hybridized to a mouse whole genome oligo expression microarray (Agilent), as previously described[6]. Analysis was performed using global mean normalization utilizing R and Bioconductor[8] as previously described[6]. Significantly changed genes were defined as at least a 2-fold increase or decrease from control and with p-values less than 0.05.

DAPI staining, confocal microscopy, and nuclear volume calculation

After sorting, $5x10^4$ to $2 x10^6$ GFP+ cells were spun onto slides for 3 min at 800 rpm (Cytospin 3) and air-dried. Cells were fixed with 4% paraformaldehyde and then nuclei were stained with 0.1 microgram/mL DAPI (4',6-Diamidino-2-Phenylindole, Dilactate, Invitrogen) for 2 min prior to mounting onto slides using ProLong® Antifade Reagent (Invitrogen). Images of erythroblast nuclei (shown in Figure 4) were taken at vertical Z-stacks using an inverted Olympus X71 (Olympus America Inc., Center Valley, PA) confocal fluorescent microscope with XYZ nanomotion stage (60x lens) and then deconvoluted using Softworx software (Applied Precision). Images were also collected at vertical Z-stacks for volume and density calculation as in [3] using an LSM 510 Meta confocal microscope system (Carl Zeiss Microscopes) (100M, NA 1.4 Plan-Apochromat lens) . Stacks of images were then processed using the isosurface module of Imaris 6.4 (Bitplane, Scientific Solutions) to obtain the estimated nuclear volume. The mean estimated nuclear volume of control cells was defined as 100%. Statistical analysis comparing knockdown nuclei to control was performed with the unpaired t-test using Prism (Graph Pad) software.

Immunofluorescence

Cells were spun onto poly-L-lysine coated coverslips in 24 well plates at 1200 rpm for 5 min, fixed in fresh 4% paraformaldehyde for 20 min, and permeabilized

by incubation in 0.25% TritonX100 for 10 min. Coverslips were then blocked with blocking buffer for 1 hr, stained with indicated antibodies (for Figures 1, 5, and S2) diluted in blocking buffer for 1h, and then washed three times with PBS. Coverslips were then re-incubated with secondary antibody (Alexa 594 anti-IgG, #A21207, Invitrogen) in PBS for 45 min, washed three times with PBS, and stained with either 0.1 microgram/mL DAPI (4',6-Diamidino-2-Phenylindole, Dilactate, Invitrogen) or with 10μM TO-PRO-3 (Life Technologies) for 30 sec, and finally mounted onto slides using ProLong® Antifade Reagent (Invitrogen). Slides were imaged at 60x lens using ZEN 2010 software (Carl Zeiss Microscopes) on the Zeiss LSM 710 Duo laser scanning confocal microscope (Carl Zeiss Microscopes) and then analyzed and processed using the Fiji[4] package of ImageJ imaging software (http://fiji.sc/wiki/index.php/Fiji).

References

1. Wong P, Hattangadi SM, Cheng AW, Frampton GM, Young RA, Lodish HF. Gene induction and repression during terminal erythropoiesis are mediated by distinct epigenetic changes. Blood.
2. Yu M, Riva L, Xie H, et al. Insights into GATA-1-mediated gene activation versus repression via genome-wide chromatin occupancy analysis. Molecular cell 2009;36:682-95.
3. Ji P, Jayapal SR, Lodish HF. Enucleation of cultured mouse fetal erythroblasts requires Rac GTPases and mDia2. Nat Cell Biol 2008;10:314-21.
4. Schindelin J, Arganda-Carreras I, Frise E, et al. Fiji: an open-source platform for biological-image analysis. Nat Methods 2012;9:676-82.
5. Flygare J, Rayon Estrada V, Shin C, Gupta S, Lodish HF. HIF1alpha synergizes with glucocorticoids to promote BFU-E progenitor self-renewal. Blood 2011;117:3435-44.
6. Hattangadi SM, Burke KA, Lodish HF. Homeodomain-interacting protein kinase 2 plays an important role in normal terminal erythroid differentiation. Blood 2010;115:4853-61.
7. Mingot JM, Bohnsack MT, Jakle U, Gorlich D. Exportin 7 defines a novel general nuclear export pathway. The EMBO journal 2004;23:3227-36.

8. Gentleman RC, Carey VJ, Bates DM, et al. Bioconductor: open software development for computational biology and bioinformatics. Genome Biol 2004;5:R80.

Figure S1.

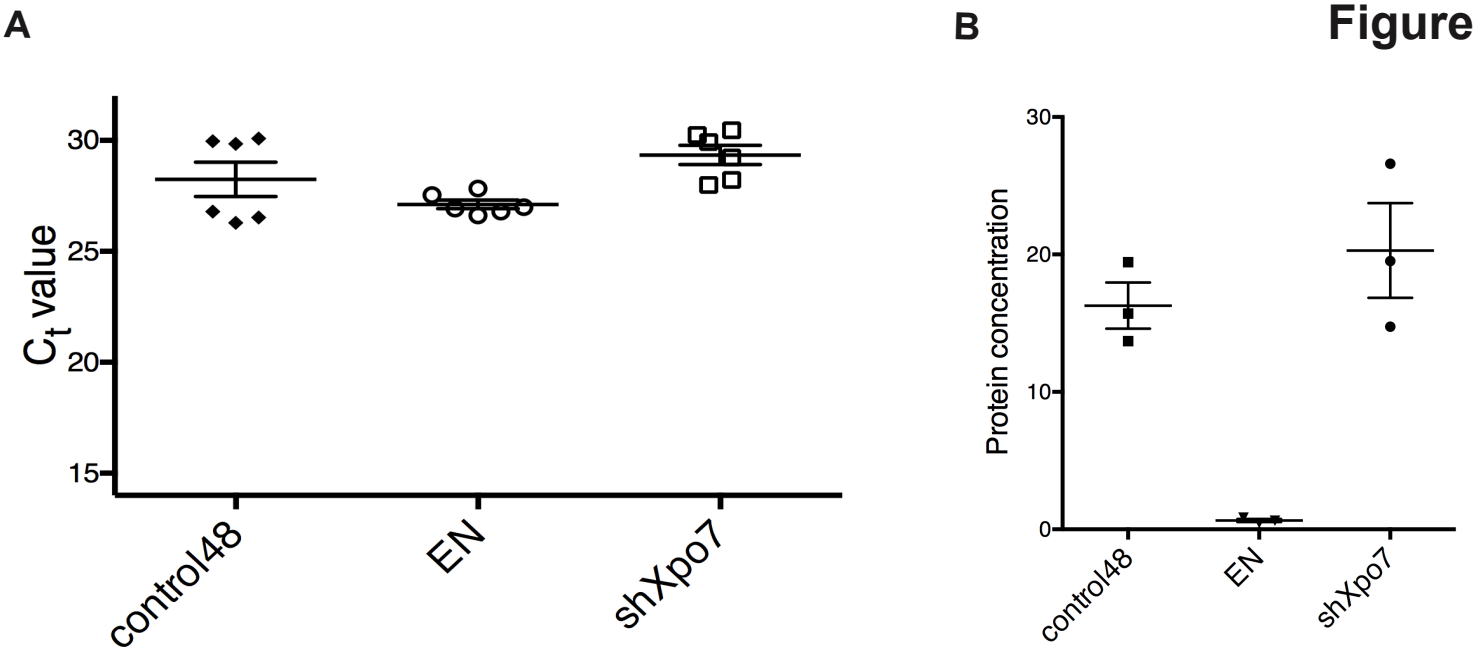
A
B
30
25
20
15
C_t value
control48
EN
shXpo7
30
20
10
0
Protein concentration
control48
EN
shXpo7

Figure S2.

A

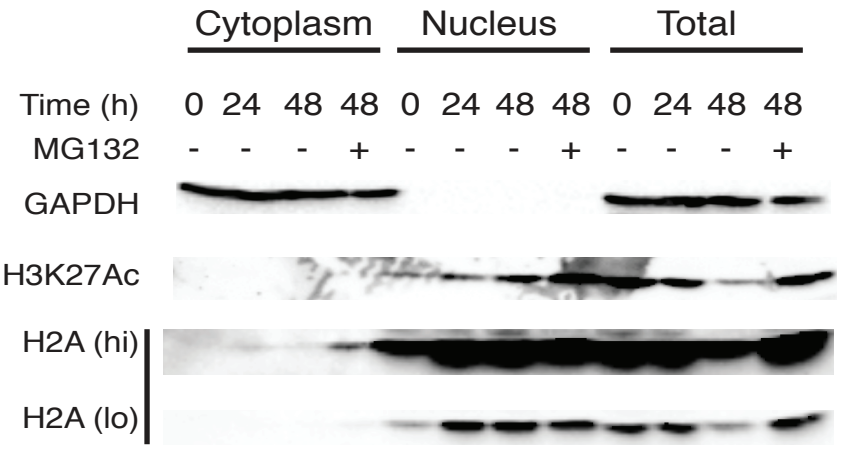

B **In-vitro Fetal Liver**

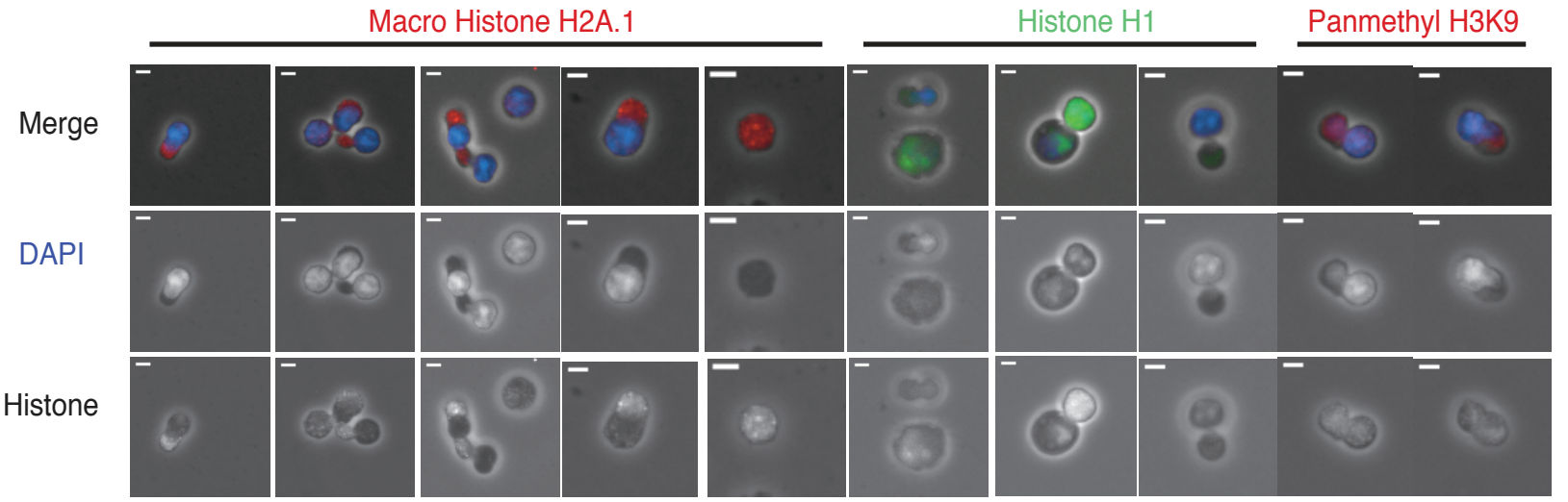

C **In-vitro Fetal Liver**

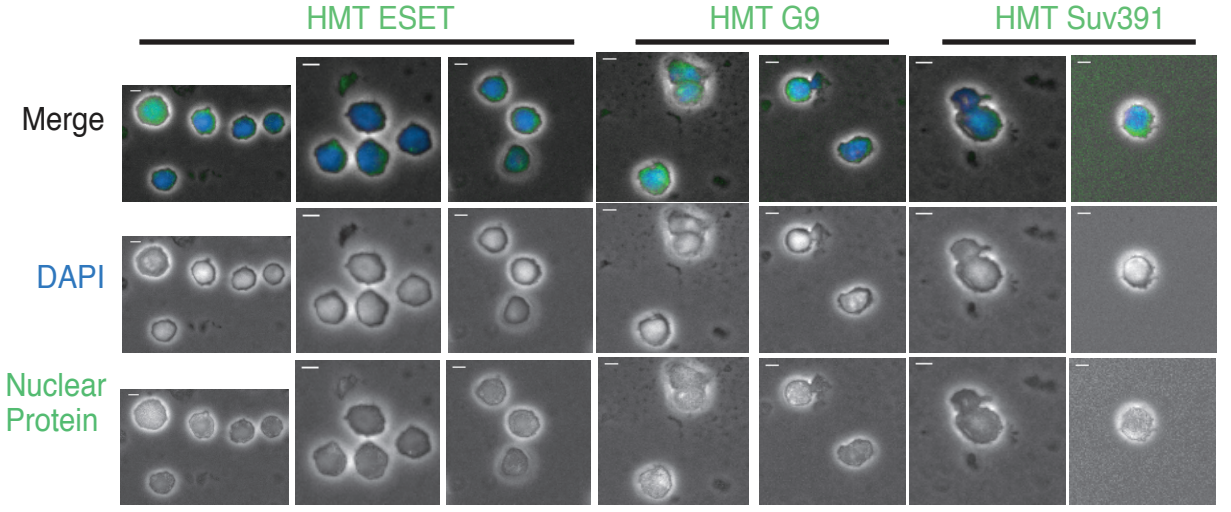

Figure S3.

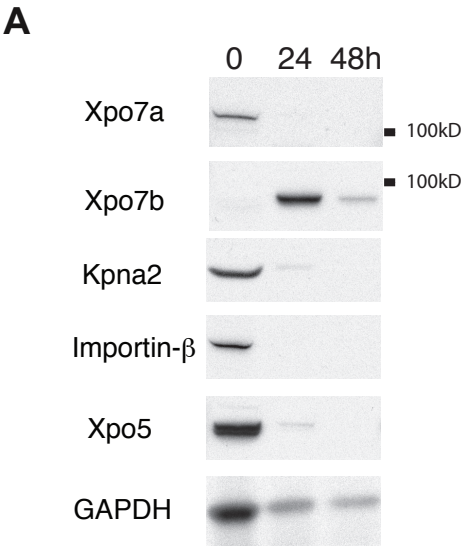
A
0
24
48h
Xpo7a
100kD
Xpo7b
100kD
Kpna2
Importin-β
Xpo5
GAPDH

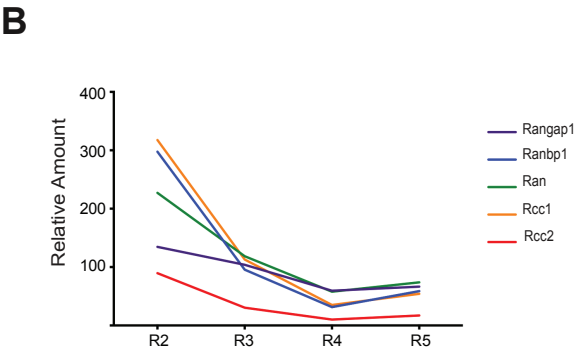
B
Relative Amount
400
300
200
100
R2
R3
R4
R5
Rangap1
Ranbp1
Ran
Rcc1
Rcc2

Figure S4.

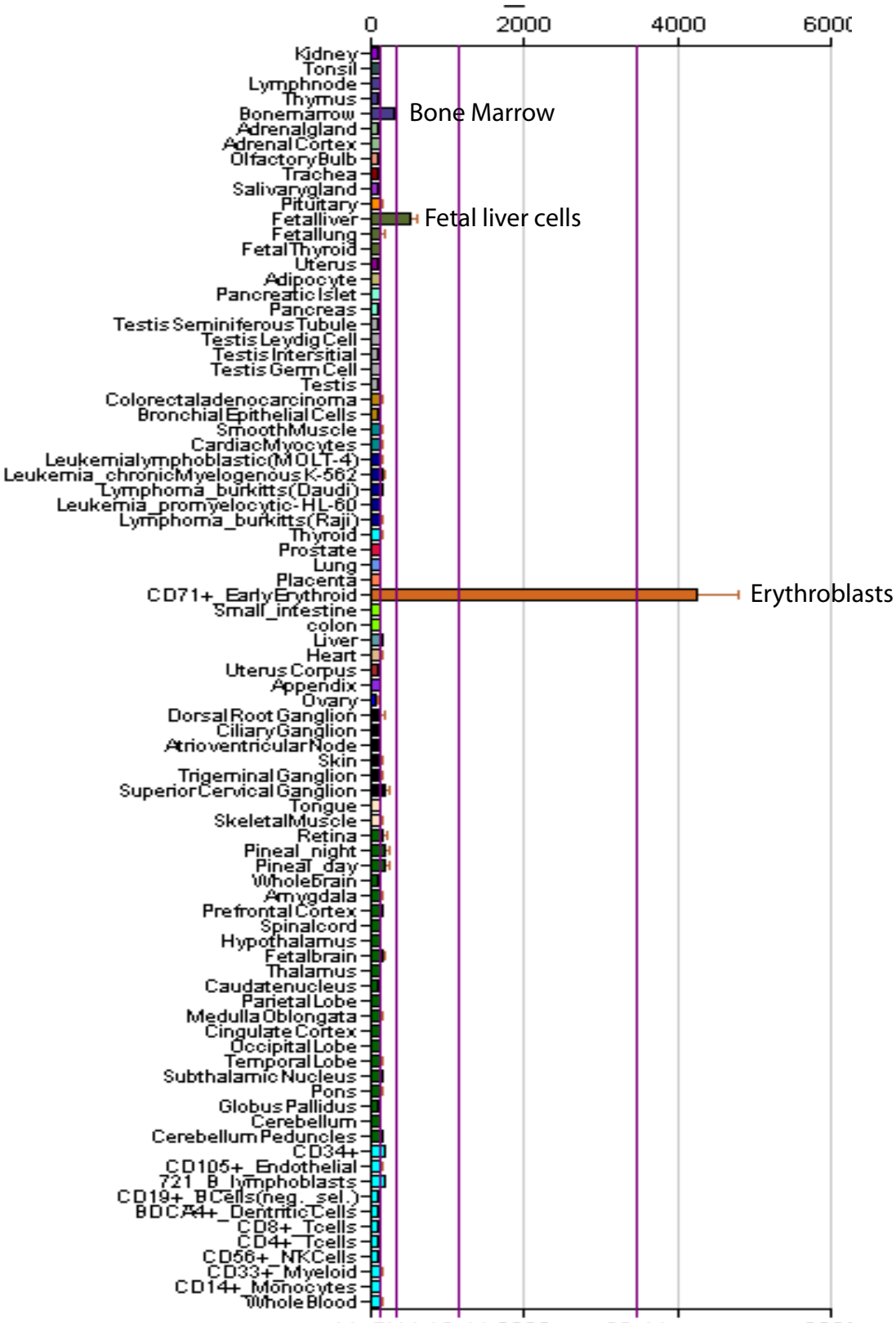
0
2000
4000
6000
Kidney
Tonsil
Lymphnode
Thymus
Bonemarrow
Adrenalgland
Adrenal Cortex
Olfactory Bulb
Trachea
Salivarygland
Pituitary
Fetalliver
Fetallung
Fetal Thyroid
Uterus
Adipocyte
Pancreatic Islet
Pancreas
Testis Seminiferous Tubule
Testis Leydig Cell
Testis Intersitial
Testis Germ Cell
Testis
Colorectaladenocarcinoma
Bronchial Epithelial Cells
SmoothMuscle
CardiacMyocytes
Leukemialymphoblastic(MOLT-4)
Leukemia_chronicMyelogenous K-562
Lymphoma_burkitts(Daudi)
Leukemia_promyelocytic-HL-60
Lymphoma_burkitts(Raji)
Thyroid
Prostate
Lung
Placenta
CD71+_EarlyErythroid
Small_intestine
colon
Liver
Heart
Uterus Corpus
Appendix
Ovary
Dorsal Root Ganglion
Ciliary Ganglion
Atrioventricular Node
Skin
Trigeminal Ganglion
Superior Cervical Ganglion
Tongue
SkeletalMuscle
Retina
Pineal_night
Pineal_day
WholeBrain
Amygdala
Prefrontal Cortex
Spinalcord
Hypothalamus
Fetalbrain
Thalamus
Caudatenucleus
Parietal Lobe
Medulla Oblongata
Cingulate Cortex
Occipital Lobe
Temporal Lobe
Subthalamic Nucleus
Pons
Globus Pallidus
Cerebellum
Cerebellum Peduncles
CD34+
CD105+_Endothelial
721_B_lymphoblasts
CD19+_BCells(neg._sel.)
BDCA4+_DentriticCells
CD8+_Tcells
CD4+_Tcells
CD56+_NKCells
CD33+_Myeloid
CD14+_Monocytes
Whole Blood
Bone Marrow
Fetal liver cells
Erythroblasts

Figure S5.

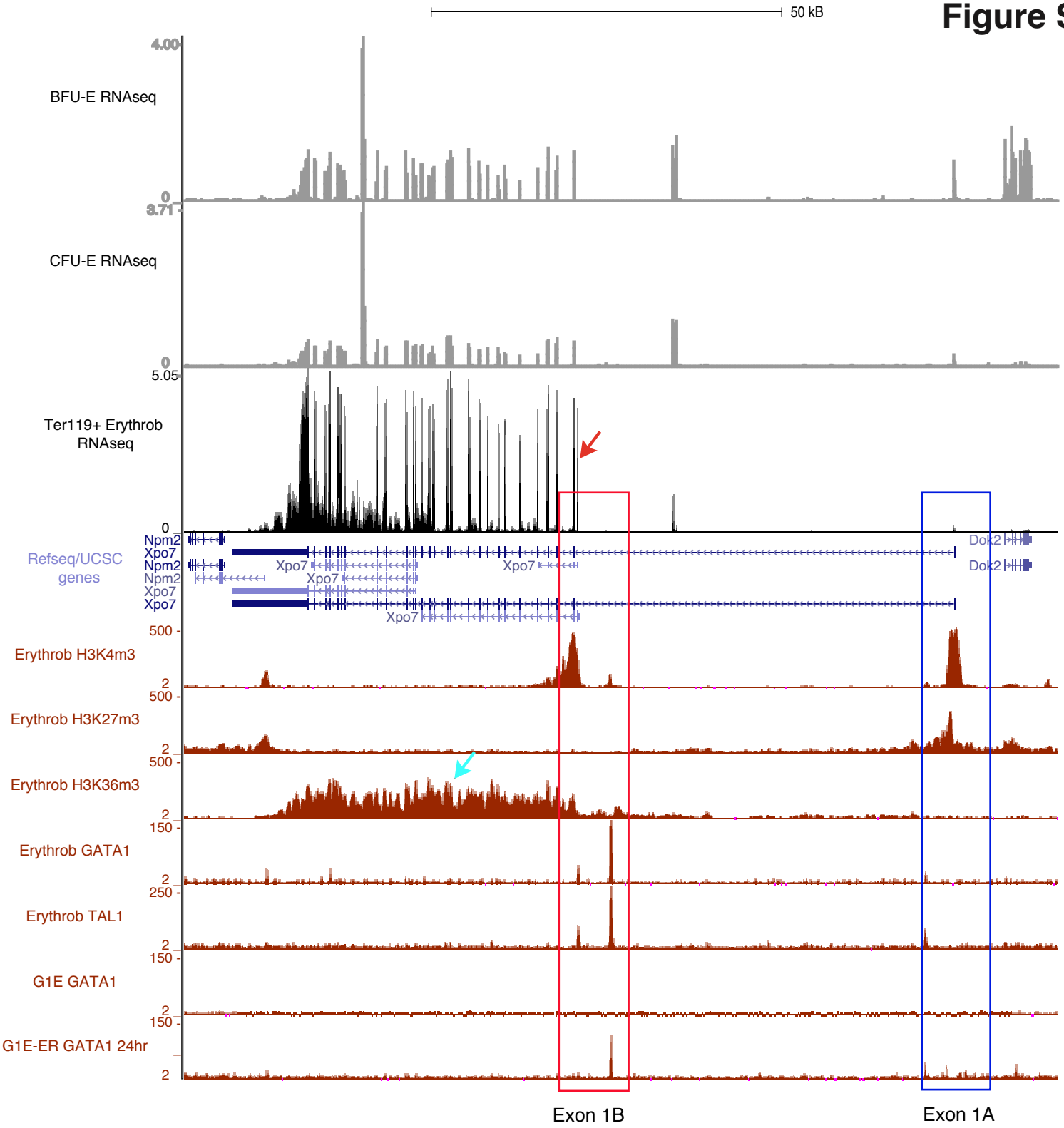
50 kB
BFU-E RNAseq
4.00
0
CFU-E RNAseq
3.71
0
Ter119+ Erythrob RNAseq
5.05
0
Refseq/UCSC genes
Npm2
Xpo7
Dok2
Erythrob H3K4m3
Erythrob H3K27m3
Erythrob H3K36m3
Erythrob GATA1
Erythrob TAL1
G1E GATA1
G1E-ER GATA1 24hr
500
150
250
2
Exon 1B
Exon 1A

Figure S6.

A

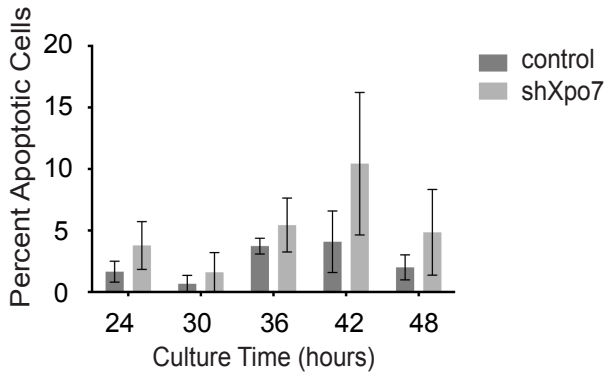
Percent Apoptotic Cells
20
15
10
5
0
24
30
36
42
48
Culture Time (hours)
control
shXpo7

B

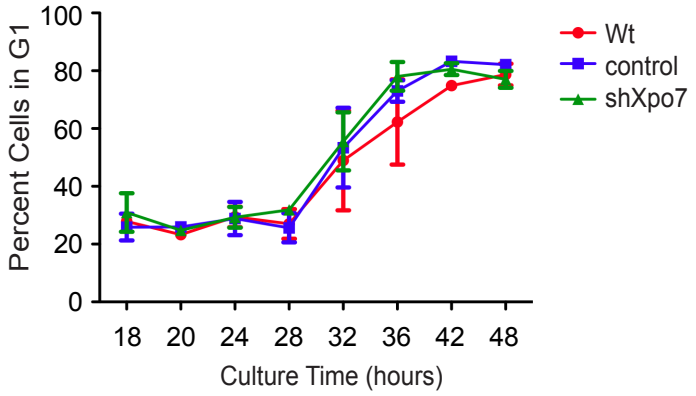
Percent Cells in G1
100
80
60
40
20
0
18
20
24
28
32
36
42
48
Culture Time (hours)
Wt
control
shXpo7

Figure S7.

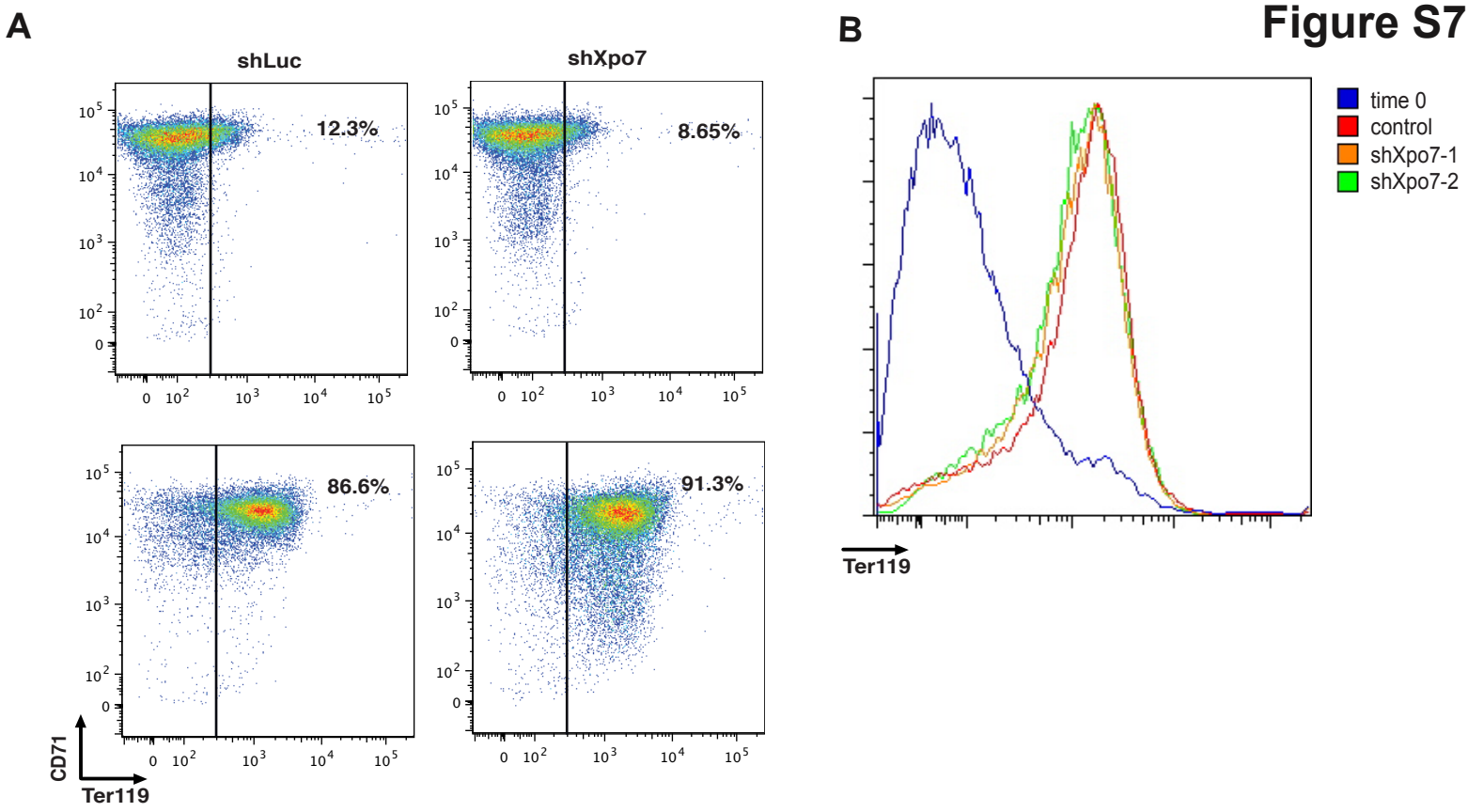
A
shLuc
shXpo7
12.3%
8.65%
86.6%
91.3%
CD71
Ter119
B
time 0
control
shXpo7-1
shXpo7-2
Ter119

Figure S8.

A

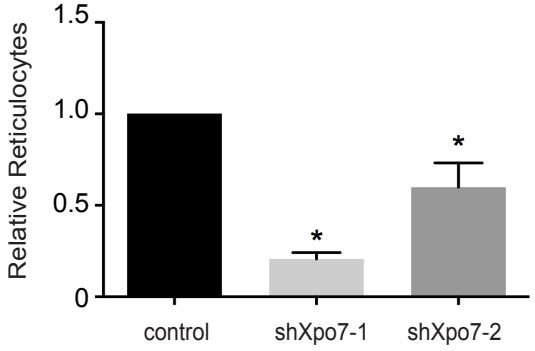
Relative Reticulocytes
1.5
1.0
0.5
0
*
*
control
shXpo7-1
shXpo7-2

B

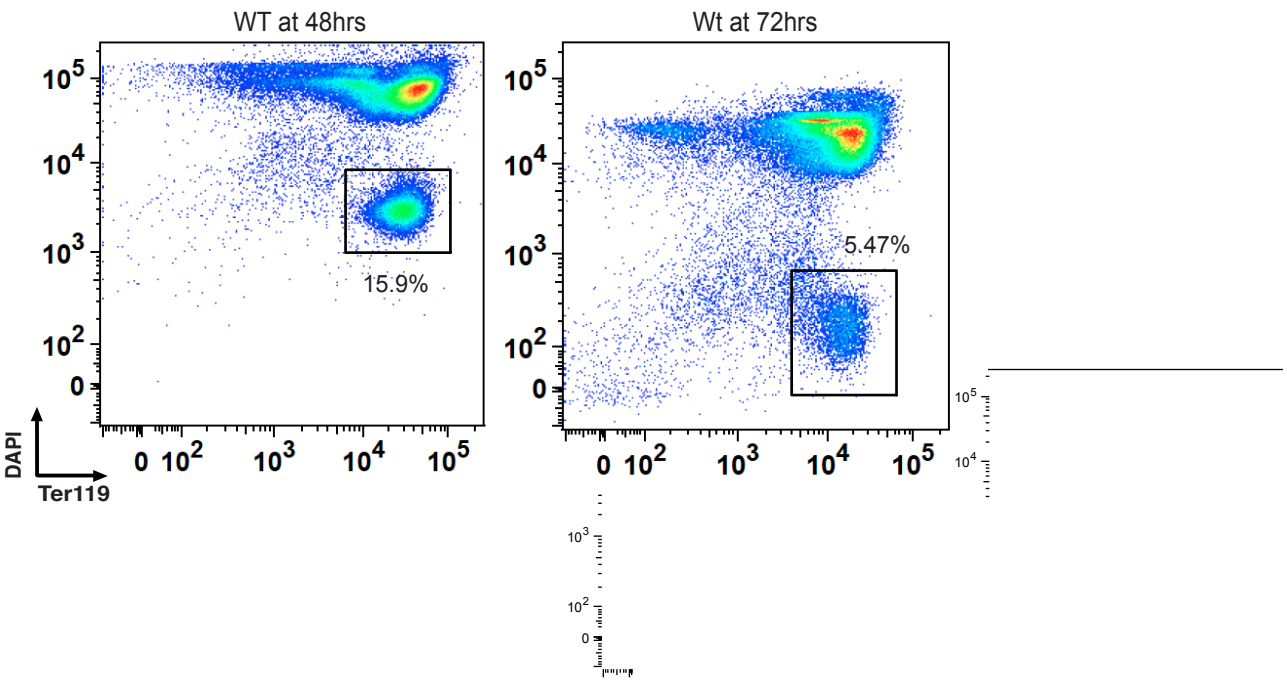
WT at 48hrs
Wt at 72hrs
15.9%
5.47%
DAPI
Ter119
0
10^2
10^3
10^4
10^5

Figure S9.